ISSN 1063-7788, Physics of Atomic Nuclei, 2011, Vol. 74, No. 4, pp. 523–536. © Pleiades Publishing, Ltd., 2011.
Original Russian Text © Yu.E. Titarenko, V.F. Batyaev, A.Yu. Titarenko, M.A. Butko, K.V. Pavlov, S.N. Florya, R.S. Tikhonov, V.M. Zhivun, A.V. Ignatyuk, S.G. Mashnik, S. Leray, A. Boudard, J. Cugnon, D. Mancusi, Y. Yariv, K. Nishihara, N. Matsuda, H. Kumawat, G. Mank, W. Gudowski, 2011, published in Yadernaya Fizika, 2011, Vol. 74, No. 4, pp. 548–560.

NUCLEI
Experiment

# Measurement and Simulation of the Cross Sections for Nuclide Production in $^{56}$Fe and $^{nat}$Cr Targets Irradiated with 0.04- to 2.6-GeV Protons

**Yu. E. Titarenko[1)*], V. F. Batyaev[1)], A. Yu. Titarenko[1)], M. A. Butko[1)], K. V. Pavlov[1)], S. N. Florya[1)], R. S. Tikhonov[1)], V. M. Zhivun[1)], A. V. Ignatyuk[2)], S. G. Mashnik[3)], S. Leray[4)], A. Boudard[4)], J. Cugnon[5)], D. Mancusi[5)], Y. Yariv[6)], K. Nishihara[7)], N. Matsuda[7)], H. Kumawat[8)], G. Mank[9)], and W. Gudowski[10)]**

Received October 7, 2010

**Abstract**—The cross sections for nuclide production in thin $^{56}$Fe and $^{nat}$Cr targets irradiated by 0.04–2.6-GeV protons are measured by direct $\gamma$ spectrometry using two $\gamma$ spectrometers with the resolutions of 1.8 and 1.7 keV for the $^{60}$Co 1332-keV $\gamma$ line. As a result, 649 yields of radioactive residual product nuclei have been obtained. The $^{27}$Al$(p,x)^{22}$Na reaction has been used as a monitor reaction. The experimental data are compared with the MCNPX (BERTINI, ISABEL), CEM03.02, INCL4.2, INCL4.5, PHITS, and CASCADE07 calculations.

**DOI:** 10.1134/S1063778811040168

## INTRODUCTION

Spallation reactions have attracted increasing attention in recent years in view of the possibility of using them in, first, electronuclear facilities developed for the transmutation of radioactive waste and, second, spallation neutron sources for fundamental and applied investigations.

The designs of such facilities requires knowledge of the cross sections for the production of important radioactive nuclides with an uncertainty of about 30%, in order to predict with a required accuracy the operational characteristics of electronuclear facilities и spallation neutron sources, including the amount of radioactive isotopes produced in target and structural materials [1].

Data on the cross sections for nuclide production in target materials of electronuclear facilities and spallation neutron sources irradiated by 0.04–2.6-GeV protons were presented in [2, 3]. Similar data for the main structural materials of electronuclear facilities were obtained in a new cycle of studies devoted to this problem [4].

The list of materials assumed to be used in the developed facilities primarily includes the "traditional" elements Cu, Fe, Cr, Co, Ni, Mn, Ta and W. In view of the request of a high-current proton accelerator for such facilities, the above list should be supplemented with Nb, which is the most promising material for creating superconducting magnets. An analysis of the behavior of structural materials under condition of irradiation shows that austenitic and ferritic/martensitic steels (e.g., 15Kh2MFA, 15Kh2NMFA, and 15Kh2NMFAA), whose main components are Fe and Cr, seem preferable [5]. For this reason, the nuclear data for Fe and Cr are particularly important.

At present, EXFOR contains 40 original works with the data on Fe and 11 works with the data on Cr, in which cumulative and independent cross sections for nuclide production in proton-induced reactions on natural samples are presented [6]. Almost all data were obtained by the direct kinematic method; i.e., thin targets were irradiated by protons with various energies ($^1$H → $^{56}$Fe, $^{nat}$Cr). On the other hand,

[1)]Institute for Theoretical and Experimental Physics, ul. Bol'shaya Cheremushkinskaya 25, Moscow, 117218 Russia.
[2)]Institute of Physics and Power Engineering, pl. Bondarenko 1, Obninsk, Kaluga oblast, 249033 Russia.
[3)]Los Alamos National Laboratory, USA.
[4)]CEA, Saclay, France.
[5)]University of Liege, Belgium.
[6)]Soreq NRC, Yavne, Israel.
[7)]JAEA, Tokai, Japan.
[8)]BARC, Mumbai, India.
[9)]IAEA, Vienna, Austria
[10)]Royal Institute of Technology, Stockholm, Sweden.
[*]E-mail: Yury.Titarenko@itep.ru

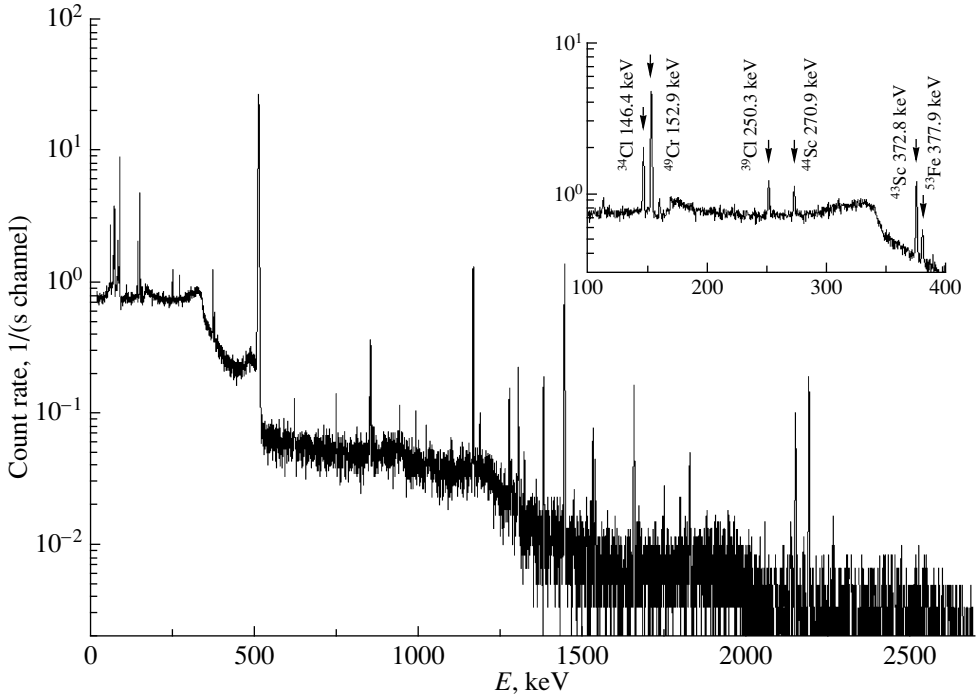


**Fig. 1.** Example of the $\gamma$ spectrum of $^{56}$Fe no. 5 for $E_p = 2.6$ GeV 1.88 h after irradiation; the measurement duration was 600 s.

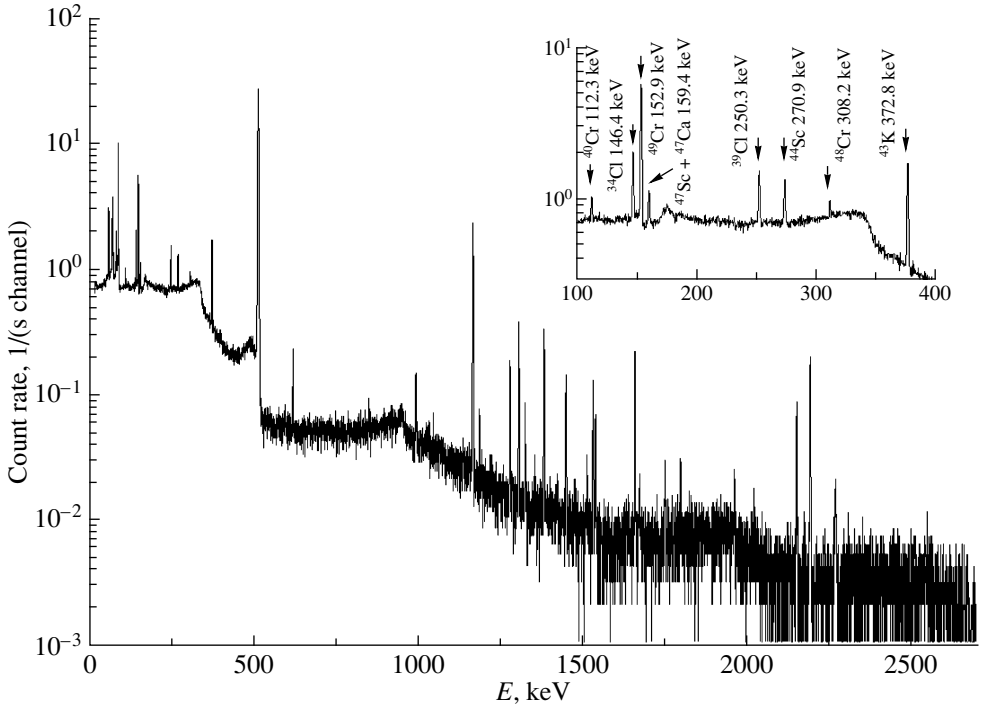


**Fig. 2.** Example of the $\gamma$ spectrum of $^{nat}$Cr no. 5 for $E_p = 2.6$ GeV 1.49 h after irradiation; the measurement duration was 900 s.

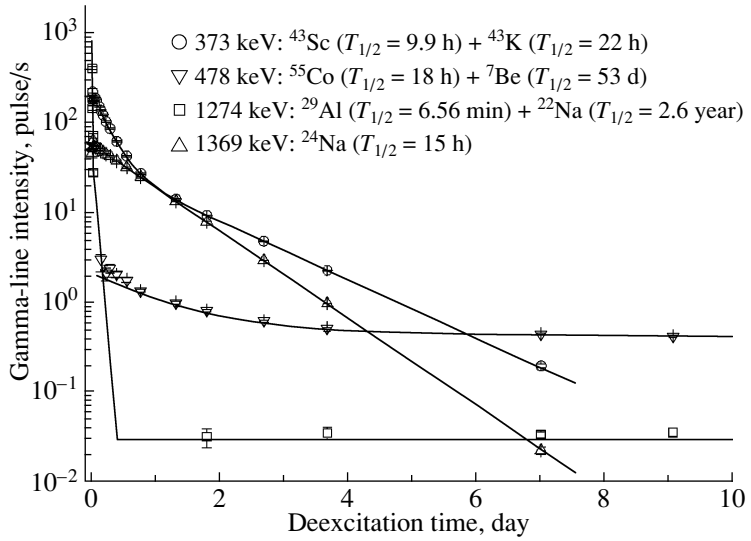


**Fig. 3.** Examples of decay curves of the products of reactions in $^{56}$Fe irradiated by 2.6-GeV protons.

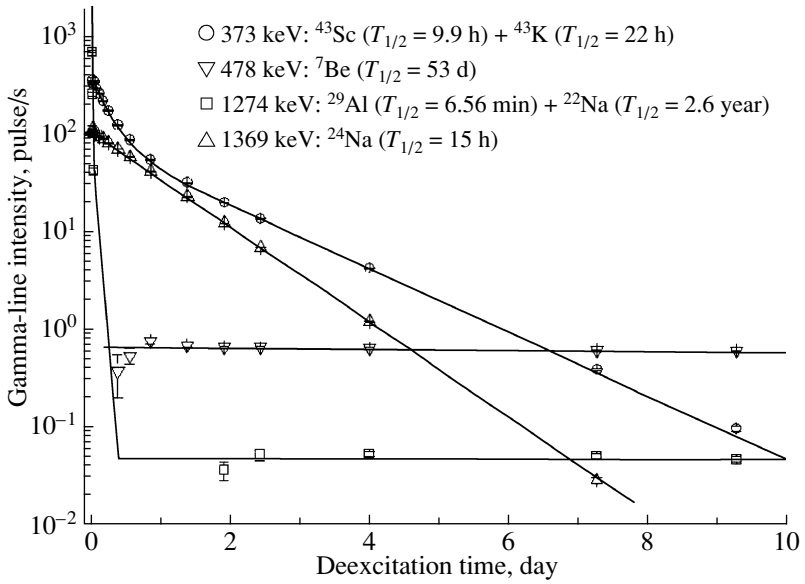


**Fig. 4.** As in Fig. 3, but for $^{nat}$Cr.

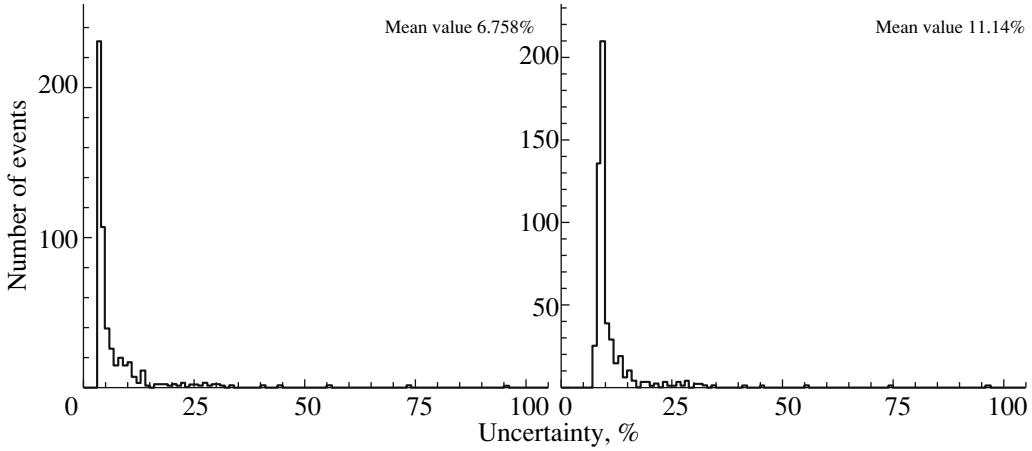


**Fig. 5.** Distribution of the uncertainties in reaction rates and cross sections for $^{56}$Fe.

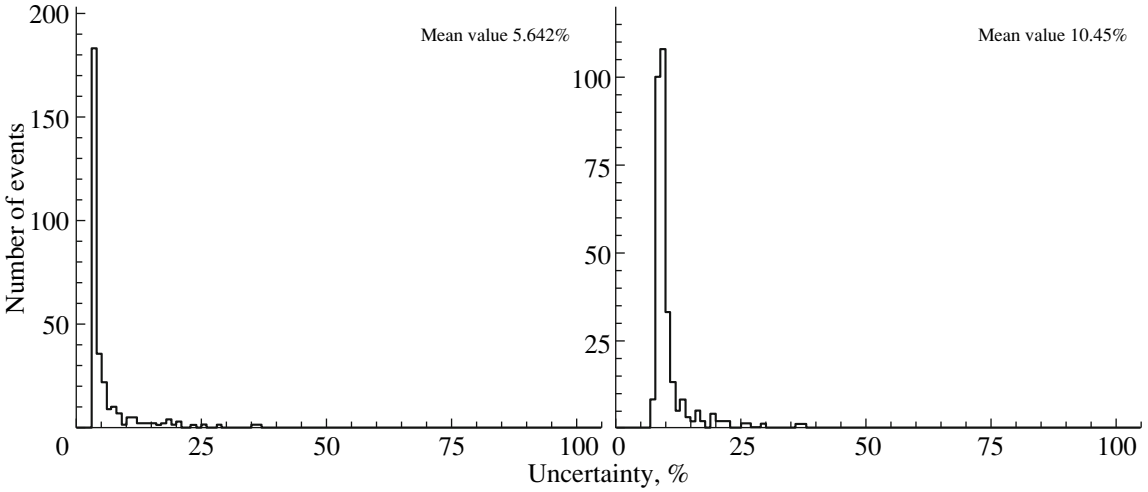


**Fig. 6.** As in Fig. 5, but for $^{nat}$Cr.

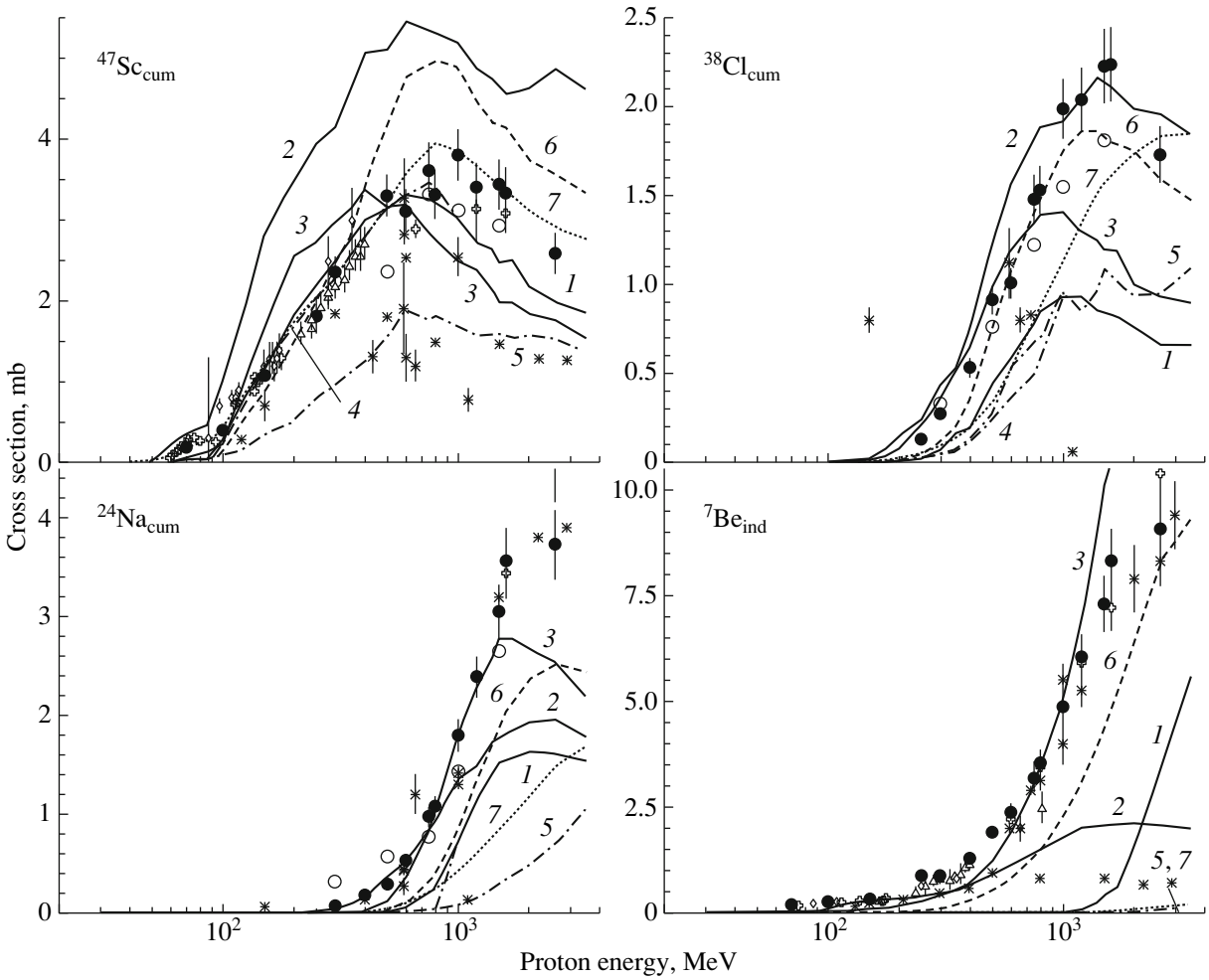


**Fig. 7.** Calculated and experimental cross sections for the $^{56}$Fe$(p, x)$ reactions. The experimental data are taken from (•) this work, (∗) [6], (○) [7], (✣) [18–22], (◇) [23], and (△) [24]. Lines *1*, *2*, *3*, *4*, *5*, *6*, and *7* represent the BERTINI, INCL4.5, CEM03.02, ISABEL, INCL4.2, PHITS, and CASCADE07 calculations, respectively.

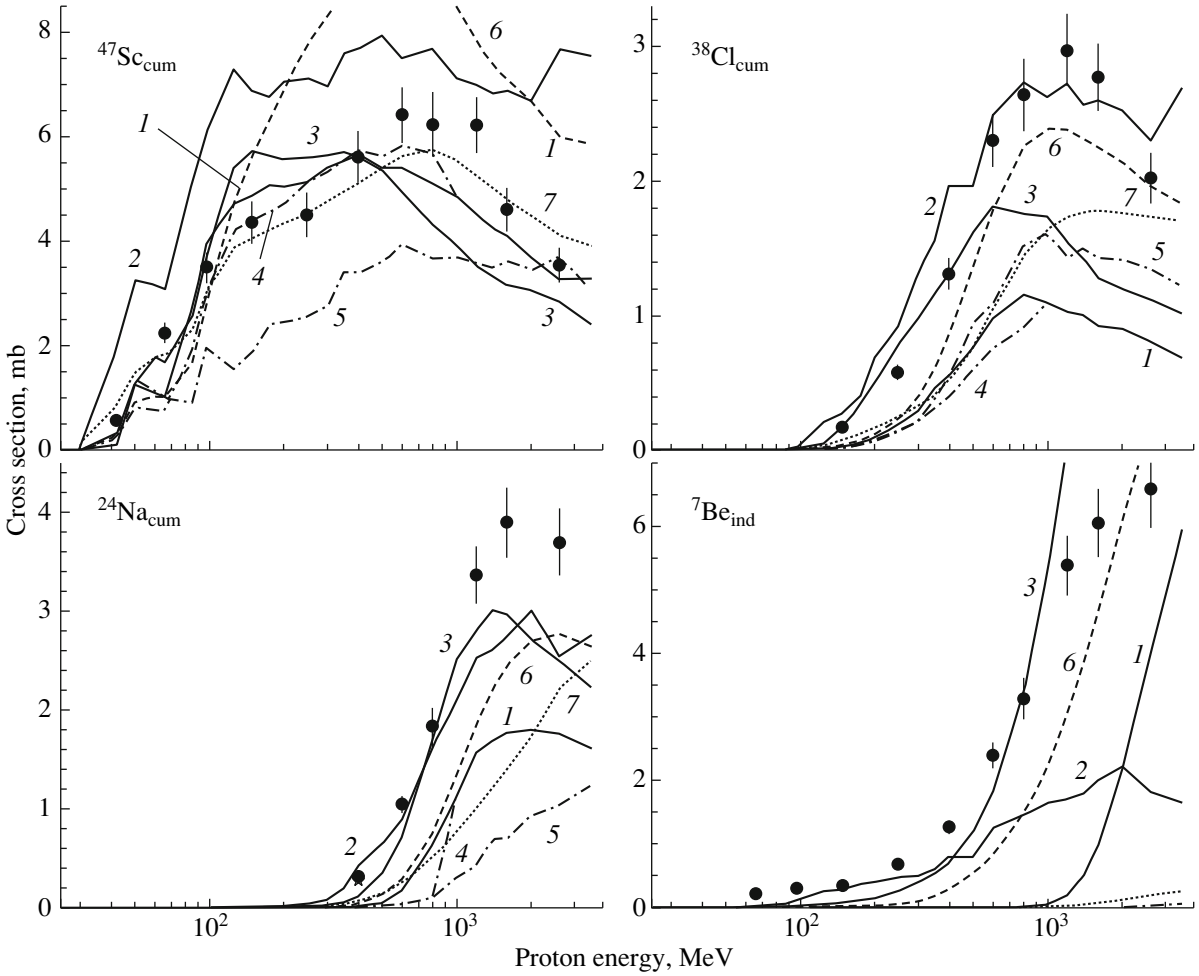


**Fig. 8.** As in Fig. 7, but for $^{nat}$Cr$(p, x)$ reactions.

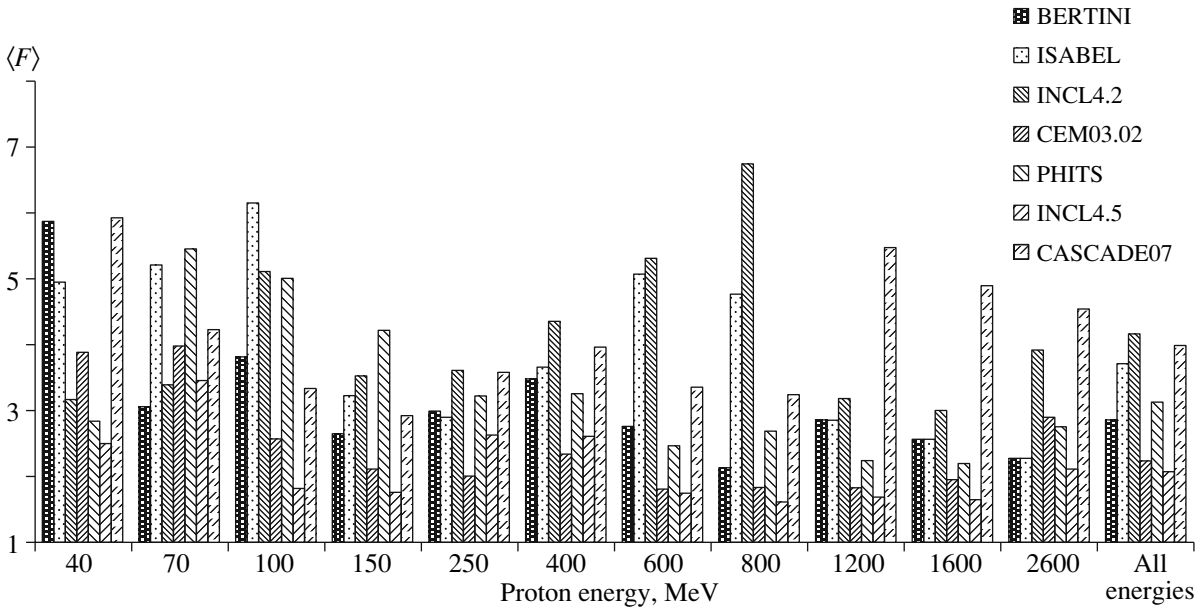


**Fig. 9.** Deviation coefficients $\langle F \rangle$ for $^{56}$Fe obtained with various codes. These data characterize the predictive powers of these codes.

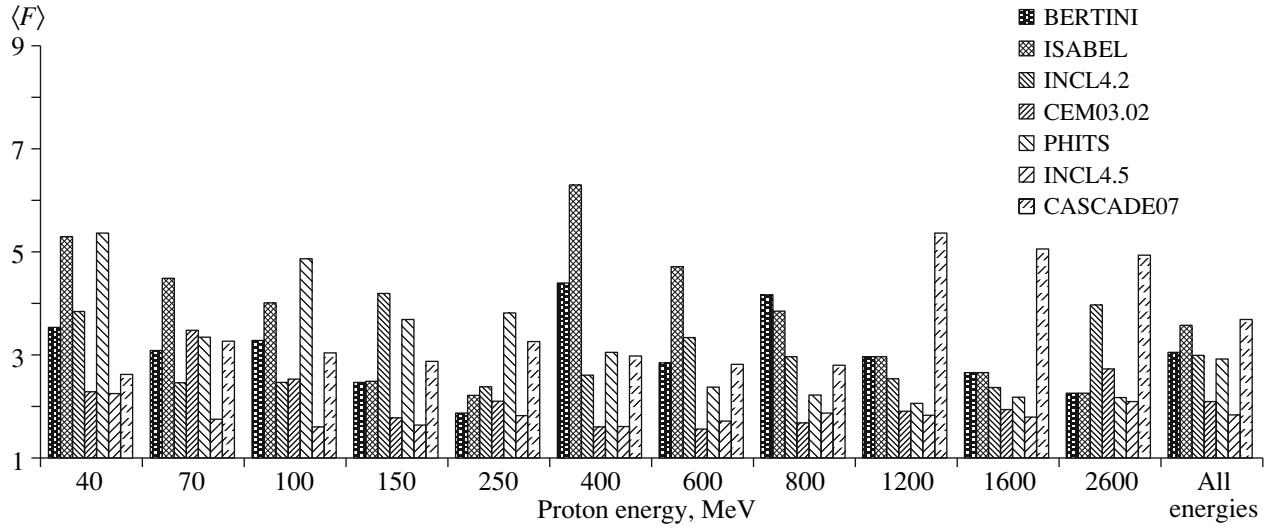


**Fig. 10.** As in Fig. 9, but for $^{nat}$Cr.

we would like to attract attention to the study reported in [7], where the independent cross sections for nuclide production on $^{56}$Fe were measured by the inverse kinematic method ($^{56}\mathrm{Fe} \to {}^{1}\mathrm{H}$) at the ion energies of 300, 500, 750, 1000, and 1500 MeV/$A$. The comparison and analysis of the data obtained in direct (ITEP) and inverse (GSI) kinematics were made in [8]. The experimental data agree within about 30%; hence, the methods used to measure them are quite reliable and both data sets can be used to verify nuclear models.

Here, we present the results of the experimental determination of the cross sections for radioactive-nuclide production in $^{56}$Fe and $^{nat}$Cr at 11 proton energies (0.04, 0.07, 0.1, 0.15, 0.25, 0.4, 0.6, 0.8, 1.2, 1.6, and 2.6 GeV); these data make it possible to obtain the experimental excitation functions and to compare them with their counterparts calculated by various codes.

## DETERMINATION OF CROSS SECTIONS

Considering the production and decay of nuclides in the single- or double-link chain of radioactive transformations of the "genetically" related parent and daughter nuclei, the independent and cumulative cross sections and the uncertainties in them can be determined from the expressions [3]

$$\sigma_i^{\mathrm{cum/ind}} = \frac{\hat{R}_i^{\mathrm{cum/ind}}}{\hat{\Phi}_{\mathrm{mon}}}, \tag{1}$$

$$\frac{\Delta\sigma_i^{\mathrm{cum/ind}}}{\sigma_i^{\mathrm{cum/ind}}} = \sqrt{\left(\frac{\Delta\hat{R}_i^{\mathrm{cum/ind}}}{\hat{R}_i^{\mathrm{cum/ind}}}\right)^2 + \left(\frac{\Delta\hat{\Phi}_{\mathrm{mon}}}{\hat{\Phi}_{\mathrm{mon}}}\right)^2},$$

where $\sigma_i^{\mathrm{cum}}$ and $\sigma_i^{\mathrm{ind}}$ are the cumulative and independent cross sections for the the parent and daughter nuclei, respectively; $\hat{R}_i^{\mathrm{cum}}$ and $\hat{R}_i^{\mathrm{ind}}$ are the sample-area-averaged cumulative and independent rates of the corresponding reactions, respectively; and $\hat{\Phi}_{\mathrm{mon}}$ are the monitor-averaged proton fluence, determined by the monitor reaction method.

The formulas for a determination of reaction rates in the regime of pulsed irradiation of samples with a proton beam whose amplitude may feature fluctuations and for the subsequent $\gamma$-spectrometric analysis have the form [3]

$$\hat{R}_1^{\mathrm{cum/ind}} = \frac{\hat{A}_1}{N_{\mathrm{tag}}\eta_1\varepsilon_1}\frac{1}{F_1}, \tag{2}$$

$$\hat{R}_1^{\mathrm{cum/ind}} = \frac{\hat{A}_2^1}{N_{\mathrm{tag}}\eta_2\varepsilon_2\nu_{12}}\frac{\lambda_2-\lambda_1}{\lambda_2}\frac{1}{F_1}, \tag{3}$$

$$\hat{R}_2^{\mathrm{ind}} = \left(\frac{\hat{A}_2^2}{F_2} + \frac{\hat{A}_2^1}{F_1}\frac{\lambda_1}{\lambda_2}\right)\frac{1}{N_{\mathrm{tag}}\eta_2\varepsilon_2}, \tag{4}$$

$$\begin{aligned}\hat{R}_2^{\mathrm{cum}} &= \hat{R}_2^{\mathrm{ind}} + \nu_{12}\hat{R}_1^{\mathrm{cum/ind}} \\ &= \left(\frac{\hat{A}_2^1}{F_1} + \frac{\hat{A}_2^2}{F_2}\right)\frac{1}{N_{\mathrm{tag}}\eta_2\varepsilon_2}.\end{aligned} \tag{5}$$

Here, $\hat{A}_1 = A_1 k_{\mu_1}$, $\hat{A}_2^1 = A_2^1 k_{\mu_2}$, and $\hat{A}_2^2 = A_2^2 k_{\mu_2}$ are the parameters determined by least-squares fitting of the experimental decay curves for the parent and daughter nuclei (indices 1 and 2 refer to the parent and daughter nuclides, respectively); $N_{\mathrm{tag}}$ is the number of nuclei in the irradiated sample; $\eta_1$ and $\eta_2$ are the absolute yields of $\gamma$ rays; $\lambda_1$ and $\lambda_2$ are the decay

**Table 1.** Parameters of irradiation of $^{nat}$Cr and $^{56}$Fe

| $^{nat}$Cr | | | | | $^{56}$Fe | | | | |
|---|---|---|---|---|---|---|---|---|---|
| Proton energy, MeV | Sample mass, mg | Monitor mass, mg | Irradiation time, min | Average proton flux, $p/(\mathrm{cm}^2\ \mathrm{s})$ $\times 10^{-10}$ | Proton energy, MeV | Sample mass, mg | Monitor mass, mg | Irradiation time, min | Average proton flux, $p/(\mathrm{cm}^2\ \mathrm{s})$ $\times 10^{-10}$ |
| $2605 \pm 8$ | 366.1 | 59.0 | 33.48 | $5.26 \pm 0.46$ | $2605 \pm 8$ | 243.3 | 59.2 | 35.13 | $4.75 \pm 0.41$ |
| $1598 \pm 4$ | 338.6 | 58.6 | 29.68 | $5.98 \pm 0.50$ | $1598 \pm 4$ | 247.4 | 59.2 | 33.67 | $5.56 \pm 0.47$ |
| $1198 \pm 3$ | 340.3 | 59.2 | 27 | $6.70 \pm 0.54$ | $1199 \pm 3$ | 243 | 59.5 | 27 | $6.62 \pm 0.53$ |
| $799 \pm 2$ | 337.4 | 59.1 | 20 | $6.88 \pm 0.64$ | $799 \pm 2$ | 245.4 | 59.1 | 20 | $6.97 \pm 0.59$ |
| $599 \pm 2$ | 328.9 | 58.3 | 29 | $6.78 \pm 0.52$ | $600 \pm 2$ | 239.8 | 58.5 | 29 | $7.99 \pm 0.64$ |
| $399 \pm 2$ | 322.2 | 48.1 | 26.33 | $5.70 \pm 0.47$ | $400 \pm 2$ | 270.4 | 47.8 | 26.33 | $6.35 \pm 0.57$ |
| $248 \pm 1$ | 339.8 | 49.2 | 29 | $7.27 \pm 0.64$ | $249 \pm 1$ | 244.7 | 47.9 | 29 | $7.22 \pm 0.51$ |
| $148 \pm 1$ | 336.9 | 49.5 | 34.75 | $3.14 \pm 0.27$ | $149 \pm 1$ | 216.4 | 49.8 | 34.75 | $3.44 \pm 0.30$ |
| $97 \pm 1$ | 338.4 | 48.1 | 35 | $3.73 \pm 0.28$ | $99 \pm 1$ | 259.2 | 48.8 | 35 | $4.07 \pm 0.31$ |
| $66 \pm 1$ | 332.3 | 24.8 | 31.5 | $5.42 \pm 0.43$ | $68 \pm 1$ | 239.6 | 49.2 | 31.5 | $5.61 \pm 0.46$ |
| $42 \pm 1$ | 330.8 | 47.6 | 36 | $2.10 \pm 0.16$ | $46 \pm 1$ | 240.1 | 48.1 | 36 | $3.12 \pm 0.22$ |
| Parameters of irradiation for the determination of the cross sections for the production of $^7$Be by 0.04–0.15-GeV protons | | | | | | | | | |
| $147 \pm 1$ | 393.9 | 48.2 | 30 | $6.82 \pm 0.53$ | $149 \pm 1$ | 401.5 | 49.6 | 30 | $6.85 \pm 0.51$ |
| $97 \pm 1$ | 350.6 | 49.5 | 31 | $5.76 \pm 0.43$ | $99 \pm 1$ | 344.3 | 48.1 | 31 | $5.66 \pm 0.42$ |
| $63 \pm 1$ | 317.0 | 48.2 | 31 | $5.50 \pm 0.38$ | $67 \pm 1$ | 477.6 | 48.3 | 31 | $5.60 \pm 0.39$ |
| $40 \pm 1$ | 361.3 | 49.2 | 46 | $2.42 \pm 0.17$ | $45 \pm 1$ | 403.9 | 48.2 | 46 | $2.10 \pm 0.15$ |

constants; $\varepsilon_1$ and $\varepsilon_2$ are the absolute efficiencies of the spectrometer at energies of $\gamma$-ray photons $E_1$ (the first nuclide) and $E_2$ (the second nuclide), respectively; $\nu_{12}$ is the branching ratio, i.e., the probability of the transition of the parent nuclide to the daughter one; and

$$F_i = \lambda_i T \frac{\sum_{j=1}^{k} I_j e^{-\lambda_i (k-j)T}}{\sum_{j=1}^{k} I_j} \quad (i = 1, 2, \mathrm{st}).$$

Here, $k$ is the number of cyclic irradiation pulses, $T$ is their repetition period, $\tau$ is the duration of one pulse, $j$ is the ordinal number of the current pulse $(1 < j < k)$, and $I$ is the integral sum of the pulses from the beam current transformer in volts.

The corrections $k_\mu$ taking into account the absorption of $\gamma$ rays in the sample material are calculated according to [2, 3].

The proton fluence is determined using the monitor reaction method. In this work, the $^{27}\mathrm{Al}(p, x)^{22}\mathrm{Na}$ reaction is used, because the excitation function of this reaction is well known for the indicated energy range [9]. In this case, the proton fluence and the uncertainty in it can be represented as

$$\hat{\Phi}_{\mathrm{mon}} = \frac{\hat{R}^{22\mathrm{Na}}}{\sigma^{22\mathrm{Na}}_{\mathrm{mon}}}, \quad (6)$$

$$\frac{\Delta\hat{\Phi}_{\mathrm{mon}}}{\hat{\Phi}_{\mathrm{mon}}} = \sqrt{\left(\frac{\Delta R^{22\mathrm{Na}}}{R^{22\mathrm{Na}}}\right)^2 + \left(\frac{\Delta\sigma^{22\mathrm{Na}}}{\sigma^{22\mathrm{Na}}}\right)^2}, \quad (7)$$

where $\sigma^{22\mathrm{Na}}$ is the cross sections for the monitor reaction, $\hat{R}^{22\mathrm{Na}}$ is the sample-area-averaged rate of the monitor reaction, and $\hat{\Phi}_{\mathrm{mon}}$ is the monitor-area-averaged proton fluence.

The required cross sections for the production of parent and daughter nuclei are calculated in accordance with Eqs. (1), where the rates of the reactions in irradiated samples are determined by Eqs. (2)–(5) and the proton fluence for the irradiated sample is determined by Eqs. (6) and (7). The formulas for uncertainties in the reaction rates were considered in detail in [3].

## IRRADIATION AND MEASUREMENTS

The samples study were irradiated with protons of energy 2.6, 1.6, 1.2, 0.8, 0.6, 0.4, 0.25, 0.15, 0.1,

**Table 2.** Experimental cross sections for radioactive-nuclide production in the $^{nat}Cr(p, x)$ reactions induced by 0.04–2.6-GeV protons

| Nuclide | Type | $T_{1/2}$ | Production cross section, mb | | | | | | | | | | |
|---|---|---|---|---|---|---|---|---|---|---|---|---|---|
| | | | $E_p = 42$ MeV | 66 MeV | 97 MeV | 148 MeV | 248 MeV | 399 MeV | 599 MeV | 799 MeV | 1198 MeV | 1599 MeV | 2605 MeV |
| $^{54}$Mn | i | 312.11 day | 0.996 | 0.430 | 0.346 | 0.250 | 0.167 | 0.153 | 0.185 | 0.167 | 0.205 | 0.177 | 0.155 |
| | | | (0.083) | (0.040) | (0.032) | (0.031) | (0.016) | (0.018) | (0.015) | (0.026) | (0.022) | (0.017) | (0.016) |
| $^{52m}$Mn | i($m$) | 21.1 min | 17.7 | 7.29 | 4.79 | 2.85 | 1.95 | 1.17 | 0.989 | 0.97 | 0.956 | 0.795 | 0.690 |
| | | | (1.4) | (0.65) | (0.66) | (0.30) | (0.40) | (0.13) | (0.099) | (0.12) | (0.095) | (0.097) | (0.075) |
| $^{52}$Mn | i | 5.591 day | 9.89 | 3.35 | 2.35 | 1.64 | 0.917 | 0.665 | 0.589 | 0.543 | 0.570 | 0.432 | 0.376 |
| | | | (0.75) | (0.29) | (0.20) | (0.16) | (0.087) | (0.059) | (0.049) | (0.054) | (0.049) | (0.039) | (0.035) |
| $^{51}$Cr | c | 27.7025 day | 329 | 152 | 120.0 | 89.9 | 58.8 | 53.9 | 52.4 | 47.8 | 48.2 | 38.6 | 31.7 |
| | | | (25) | (13) | (10.0) | (8.5) | (5.5) | (4.8) | (4.4) | (4.7) | (4.2) | (3.4) | (2.9) |
| $^{49}$Cr | c | 42.3 min | 10.02 | 30.7 | 21.0 | 14.8 | 9.80 | 7.89 | 6.96 | 5.86 | 5.31 | 4.11 | 3.23 |
| | | | (0.80) | (2.8) | (1.9) | (1.6) | (0.98) | (0.73) | (0.61) | (0.61) | (0.49) | (0.48) | (0.38) |
| $^{48}$Cr | c | 21.56 h | 1.65 | 1.57 | 2.44 | 1.81 | 1.21 | 1.000 | 0.869 | 0.742 | 0.628 | 0.491 | 0.367 |
| | | | (0.13) | (0.14) | (0.21) | (0.18) | (0.11) | (0.090) | (0.074) | (0.075) | (0.056) | (0.044) | (0.035) |
| $^{48}$V | c | 15.9735 day | 46.3 | 33.3 | 50.9 | 42.2 | 30.1 | 27.2 | 24.6 | 21.0 | 19.2 | 16.0 | 12.1 |
| | | | (3.5) | (2.8) | (4.3) | (4.0) | (2.8) | (2.4) | (2.1) | (2.1) | (1.7) | (1.4) | (1.1) |
| $^{48}$Sc | i | 43.67 h | 0.014 | 0.110 | 0.514 | 0.639 | 0.742 | 1.010 | 1.27 | 1.34 | 1.34 | 1.130 | 0.870 |
| | | | (0.002) | (0.011) | (0.047) | (0.065) | (0.071) | (0.090) | (0.11) | (0.14) | (0.12) | (0.100) | (0.080) |
| $^{47}$Sc | i | 3.3492 day | – | – | – | 4.31 | 4.44 | 5.51 | 6.34 | 6.21 | 6.12 | 4.50 | 3.45 |
| | | | | | | (0.41) | (0.42) | (0.49) | (0.53) | (0.62) | (0.53) | (0.40) | (0.32) |
| $^{47}$Sc | c | 3.3492 day | 0.578 | 2.24 | 3.50 | 4.38 | 4.50 | 5.62 | 6.41 | 6.23 | 6.21 | 4.61 | 3.54 |
| | | | (0.043) | (0.19) | (0.30) | (0.42) | (0.42) | (0.50) | (0.54) | (0.62) | (0.54) | (0.41) | (0.33) |
| $^{46}$Sc | i($m+g$) | 83.79 day | 0.266 | 9.61 | 10.50 | 12.7 | 12.3 | 14.4 | 15.5 | 14.2 | 13.4 | 11.10 | 8.28 |
| | | | (0.023) | (0.84) | (0.90) | (1.2) | (1.2) | (1.3) | (1.3) | (1.4) | (1.2) | (1.00) | (0.79) |
| $^{44m}$Sc | i($m$) | 58.61 h | 0.154 | 1.58 | 6.48 | 7.51 | 7.72 | 8.93 | 9.79 | 8.81 | 8.11 | 6.14 | 4.49 |
| | | | (0.012) | (0.13) | (0.56) | (0.72) | (0.72) | (0.79) | (0.82) | (0.87) | (0.72) | (0.55) | (0.42) |
| $^{44}$Sc | i | 3.97 h | 0.284 | 2.59 | 9.45 | 10.65 | 10.7 | 13.4 | 14.3 | 12.8 | 11.39 | 9.78 | 7.05 |
| | | | (0.021) | (0.22) | (0.85) | (1.00) | (1.2) | (1.2) | (1.2) | (1.3) | (1.00) | (0.87) | (0.66) |
| $^{44}$Sc | i($m+g$) | 3.97 h | 0.433 | 4.13 | 16.5 | 18.4 | 20.4 | 22.3 | 24.4 | 21.5 | 19.3 | 16.0 | 11.6 |
| | | | (0.038) | (0.35) | (1.6) | (1.8) | (1.9) | (2.0) | (2.0) | (2.2) | (1.7) | (1.4) | (1.1) |
| $^{43}$Sc | c | 3.891 h | 0.124 | 1.27 | 2.46 | 4.70 | 5.50 | 6.82 | 7.43 | 6.75 | 6.08 | 4.82 | 3.47 |
| | | | (0.012) | (0.12) | (0.22) | (0.48) | (0.54) | (0.65) | (0.67) | (0.71) | (0.59) | (0.46) | (0.35) |
| $^{47}$Ca | c | 4.536 day | – | – | – | 0.026 | 0.051 | 0.079 | 0.097 | 0.107 | 0.135 | 0.112 | 0.089 |
| | | | | | | (0.008) | (0.009) | (0.013) | (0.025) | (0.040) | (0.018) | (0.011) | (0.009) |
| $^{45}$K | c | 17.3 min | – | – | – | – | – | 0.049 | 0.091 | 0.092 | 0.098 | 0.086 | 0.074 |
| | | | | | | | | (0.011) | (0.013) | (0.014) | (0.016) | (0.012) | (0.010) |

**Table 2.** (Contd.)

| Nuclide | Type | $T_{1/2}$ | Production cross section, mb | | | | | | | | | | |
|---|---|---|---|---|---|---|---|---|---|---|---|---|---|
| | | | $E_p = 42$ MeV | 66 MeV | 97 MeV | 148 MeV | 248 MeV | 399 MeV | 599 MeV | 799 MeV | 1198 MeV | 1599 MeV | 2605 MeV |
| $^{44}$K | c* | 22.13 min | – | – | – | – | – | 0.246 | 0.362 | 0.395 | 0.444 | 0.373 | 0.304 |
| | | | | | | | | (0.048) | (0.061) | (0.082) | (0.088) | (0.078) | (0.060) |
| $^{43}$K | c | 22.3 h | – | 0.034 | 0.195 | 0.570 | 0.961 | 1.57 | 2.21 | 2.33 | 2.26 | 1.83 | 1.42 |
| | | | | (0.003) | (0.017) | (0.054) | (0.090) | (0.14) | (0.18) | (0.23) | (0.20) | (0.16) | (0.13) |
| $^{42}$K | i | 12.360 h | – | 0.021 | 1.100 | 2.08 | 3.28 | 5.31 | 7.22 | 7.32 | 6.94 | 5.89 | 4.34 |
| | | | | (0.003) | (0.090) | (0.20) | (0.31) | (0.47) | (0.60) | (0.73) | (0.60) | (0.52) | (0.40) |
| $^{38}$K | i | 7.636 min | – | – | – | 0.105 | 0.311 | 0.672 | 1.03 | 1.03 | 0.75 | 1.05 | 0.787 |
| | | | | | | (0.024) | (0.069) | (0.069) | (0.10) | (0.11) | (0.10) | (0.13) | (0.096) |
| $^{41}$Ar | c | 109.34 min | – | – | 0.045 | 0.155 | 0.360 | 0.714 | 1.091 | 1.18 | 1.26 | 1.130 | 0.873 |
| | | | | | (0.004) | (0.015) | (0.033) | (0.064) | (0.090) | (0.12) | (0.11) | (0.100) | (0.081) |
| $^{39}$Cl | c | 55.6 min | – | – | – | 0.043 | 0.144 | 0.361 | 0.630 | 0.732 | 0.846 | 0.757 | 0.585 |
| | | | | | | (0.006) | (0.014) | (0.034) | (0.054) | (0.074) | (0.075) | (0.078) | (0.062) |
| $^{38}$Cl | i($m+g$) | 37.24 min | – | – | – | – | 0.588 | 1.28 | 2.25 | 2.57 | 2.90 | 2.69 | 1.94 |
| | | | | | | | (0.059) | (0.12) | (0.19) | (0.26) | (0.27) | (0.25) | (0.18) |
| $^{38}$Cl | c | 37.24 min | – | – | 0.045 | 0.171 | 0.578 | 1.30 | 2.30 | 2.64 | 2.97 | 2.77 | 2.02 |
| | | | | | (0.006) | (0.018) | (0.056) | (0.12) | (0.20) | (0.27) | (0.27) | (0.25) | (0.19) |
| $^{34m}$Cl | i($m$) | 32.00 min | – | – | – | 0.033 | 0.140 | 0.400 | 0.791 | 0.948 | 1.141 | 1.05 | 0.744 |
| | | | | | | (0.012) | (0.017) | (0.036) | (0.067) | (0.095) | (0.099) | (0.14) | (0.085) |
| $^{38}$S | c | 170.3 min | – | – | – | – | 0.007 | 0.024 | 0.050 | 0.072 | 0.077 | 0.081 | 0.064 |
| | | | | | | | (0.002) | (0.003) | (0.005) | (0.008) | (0.008) | (0.009) | (0.008) |
| $^{29}$Al | c | 6.56 min | – | – | – | – | – | 0.389 | 1.21 | 1.86 | 2.61 | 3.15 | 2.57 |
| | | | | | | | | (0.039) | (0.10) | (0.19) | (0.24) | (0.29) | (0.24) |
| $^{28}$Mg | c | 20.915 h | – | – | – | – | 0.007 | 0.042 | 0.143 | 0.244 | 0.420 | 0.467 | 0.421 |
| | | | | | | | (0.001) | (0.004) | (0.012) | (0.024) | (0.037) | (0.042) | (0.039) |
| $^{27}$Mg | c | 9.458 min | – | – | – | – | – | 0.146 | 0.559 | 0.915 | 1.35 | 1.79 | 1.57 |
| | | | | | | | | (0.022) | (0.050) | (0.092) | (0.13) | (0.16) | (0.15) |
| $^{24}$Na | c | 14.9590 h | – | – | – | 0.012 | 0.061 | 0.308 | 1.040 | 1.83 | 3.36 | 3.89 | 3.69 |
| | | | | | | (0.002) | (0.006) | (0.027) | (0.090) | (0.18) | (0.29) | (0.35) | (0.34) |
| $^{22}$Na | c | 2.6019 yr | – | – | – | – | – | 0.216 (0.035) | 0.659 (0.064) | 1.09 (0.11) | 2.06 (0.18) | 2.55 (0.23) | 2.44 (0.23) |
| $^{7}$Be | i | 53.29 day | 0.056 | 0.212 | 0.297 | 0.348 | 0.676 | 1.26 | 2.39 | 3.28 | 5.38 | 6.04 | 6.58 |
| | | | (0.010)* | (0.022)** | (0.028) | (0.032) | (0.069) | (0.11) | (0.20) | (0.33) | (0.46) | (0.54) | (0.61) |

* At 40 MeV.
** At 63 MeV.

**Table 3.** Experimental cross sections for radioactive-nuclide production in the $^{56}$Fe$(p, x)$ reactions induced by 0.04- to 2.6-GeV protons

| Nuclide | Type | $T_{1/2}$ | Production cross section, mb | | | | | | | | | | |
|---|---|---|---|---|---|---|---|---|---|---|---|---|---|
| | | | $E_p = 46$ MeV | 68 MeV | 99 MeV | 149 MeV | 249 MeV | 400 MeV | 600 MeV | 799 MeV | 1199 MeV | 1599 MeV | 2605 MeV |
| $^{57}$Co | i | 271.74 day | 0.077 (0.010) | 0.073 (0.007) | 0.079 (0.008) | 0.080 (0.010) | 0.075 (0.008) | 0.104 (0.020) | 0.152 (0.015) | 0.194 (0.019) | 0.277 (0.024) | 0.343 (0.031) | 0.321 (0.030) |
| $^{56}$Co | i | 77.233 day | 11.00 (0.90) | 6.36 (0.56) | 4.42 (0.38) | 2.68 (0.25) | 1.61 (0.12) | 1.14 (0.11) | 0.922 (0.080) | 0.914 (0.084) | 1.030 (0.090) | 1.050 (0.100) | 0.854 (0.080) |
| $^{55}$Co | i | 17.53 h | 8.85 (0.78) | 5.12 (0.47) | 3.44 (0.34) | 2.08 (0.23) | 1.22 (0.13) | 0.75 (0.10) | 0.451 (0.041) | 0.391 (0.038) | 0.354 (0.045) | 0.358 (0.041) | 0.268 (0.033) |
| $^{53}$Fe | c* | 8.51 min | 3.56 (0.40) | 15.1 (1.7) | 9.1 (1.1) | 6.92 (0.85) | 5.07 (0.54) | 3.90 (0.53) | 2.88 (0.34) | 2.55 (0.34) | 2.51 (0.30) | 2.46 (0.39) | 1.84 (0.20) |
| $^{52}$Fe | c | 8.275 h | 0.035 (0.026) | 0.96 (0.13) | 1.09 (0.15) | 0.96 (0.12) | 0.76 (0.16) | 0.560 (0.070) | 0.392 (0.055) | 0.354 (0.048) | 0.294 (0.029) | 0.296 (0.032) | 0.229 (0.031) |
| $^{56}$Mn | c | 2.5789 h | 0.110 (0.011) | 0.128 (0.014) | 0.151 (0.014) | 0.150 (0.017) | 0.225 (0.023) | 0.393 (0.043) | 0.534 (0.050) | 0.714 (0.067) | 0.897 (0.084) | 0.921 (0.085) | 0.735 (0.071) |
| $^{54}$Mn | i | 312.11 day | 148 (12) | 72.7 (6.4) | 64.0 (5.6) | 48.0 (4.5) | 42.1 (3.3) | 39.4 (3.8) | 36.4 (3.2) | 37.0 (3.4) | 38.6 (3.3) | 40.3 (3.6) | 31.3 (2.9) |
| $^{52m}$Mn | i($m$) | 21.1 min | 4.54 (0.38) | 13.6 (1.2) | 15.8 (1.6) | 13.3 (1.5) | 10.3 (3.1) | 8.92 (0.87) | 7.81 (0.70) | 7.28 (0.69) | 7.39 (0.72) | 6.59 (0.63) | 5.18 (0.50) |
| $^{52m}$Mn | c | 21.1 min | 4.67 (0.39) | 14.4 (1.6) | 17.0 (1.7) | 14.4 (1.7) | 11.5 (3.2) | 9.57 (0.93) | 8.30 (0.74) | 7.70 (0.72) | 7.74 (0.75) | 6.95 (0.66) | 5.45 (0.52) |
| $^{52}$Mn | c | 5.591 day | 6.02 (0.50) | 25.4 (2.3) | 26.2 (2.3) | 18.7 (1.8) | 14.3 (1.1) | 12.1 (1.2) | 9.77 (0.94) | 9.00 (0.89) | 8.45 (0.78) | 8.66 (0.79) | 6.41 (0.60) |
| $^{51}$Cr | c | 27.7025 day | 79.3 (6.4) | 30.5 (2.7) | 66.1 (5.8) | 55.4 (5.3) | 49.6 (3.9) | 46.2 (4.4) | 39.7 (3.5) | 37.5 (3.4) | 35.8 (3.1) | 35.9 (3.2) | 26.9 (2.5) |
| $^{49}$Cr | c | 42.3 min | 0.058 (0.011) | 2.73 (0.28) | 6.48 (0.60) | 6.90 (0.69) | 7.03 (0.58) | 7.11 (0.72) | 6.23 (0.57) | 5.75 (0.55) | 5.35 (0.49) | 5.08 (0.51) | 3.81 (0.40) |
| $^{48}$Cr | c | 21.56 h | 0.033 (0.004) | 0.022 (0.002) | 0.666 (0.060) | 0.710 (0.068) | 0.840 (0.066) | 0.916 (0.089) | 0.834 (0.074) | 0.767 (0.073) | 0.698 (0.063) | 0.699 (0.064) | 0.485 (0.047) |
| $^{48}$V | c | 15.9735 day | 2.15 (0.18) | 1.73 (0.15) | 16.1 (1.4) | 16.8 (1.6) | 19.2 (1.5) | 20.0 (1.9) | 19.9 (1.7) | 19.2 (1.7) | 17.9 (1.5) | 17.4 (1.6) | 12.7 (1.2) |
| $^{48}$Sc | i | 43.67 h | 0.033 (0.037) | 0.027 (0.030) | 0.084 (0.012) | 0.152 (0.015) | 0.261 (0.026) | 0.403 (0.043) | 0.490 (0.044) | 0.505 (0.049) | 0.558 (0.059) | 0.583 (0.061) | 0.417 (0.042) |
| $^{47}$Sc | i | 3.3492 day | – | – | – | – | 1.80 (0.14) | – | 3.06 (0.27) | 3.27 (0.30) | 3.35 (0.29) | 3.40 (0.31) | 2.54 (0.24) |
| $^{47}$Sc | c | 3.3492 day | – | 0.194 (0.017) | 0.400 (0.035) | 1.080 (0.100) | 1.81 (0.14) | – | 3.11 (0.28) | 3.32 (0.31) | 3.41 (0.30) | 3.33 (0.32) | 2.58 (0.24) |
| $^{46}$Sc | i($m + g$) | 83.79 day | 0.116 (0.027) | 0.083 (0.018) | 1.64 (0.15) | 3.20 (0.31) | 5.31 (0.41) | 7.81 (0.75) | 8.84 (0.77) | 9.33 (0.85) | 9.39 (0.81) | 9.39 (0.85) | 6.84 (0.64) |
| $^{44m}$Sc | i($m$) | 58.61 h | – | 0.105 (0.010) | 0.516 (0.046) | 1.90 (0.19) | 4.17 (0.33) | 5.98 (0.62) | 7.70 (0.68) | 8.35 (0.78) | 8.30 (0.73) | 8.24 (0.77) | 5.94 (0.57) |
| $^{44}$Sc | i | 3.97 h | – | 0.191 (0.017) | 0.645 (0.059) | 2.32 (0.23) | 4.56 (0.39) | 6.83 (0.68) | 8.61 (0.75) | 9.23 (0.91) | 9.61 (0.87) | 9.17 (0.84) | 6.50 (0.61) |
| $^{44}$Sc | i($m + g$) | 3.97 h | – | 0.290 (0.025) | 1.08 (0.15) | 4.16 (0.39) | 8.65 (0.66) | 12.4 (1.2) | 16.2 (1.4) | 17.5 (1.6) | 17.7 (1.6) | 17.1 (1.5) | 12.4 (1.1) |

**Table 3.** (Contd.)

| Nuclide | Type | $T_{1/2}$ | Production cross section, mb | | | | | | | | | | |
|---|---|---|---|---|---|---|---|---|---|---|---|---|---|
| | | | $E_p = 46$ MeV | 68 MeV | 99 MeV | 149 MeV | 249 MeV | 400 MeV | 600 MeV | 799 MeV | 1199 MeV | 1599 MeV | 2605 MeV |
| $^{43}$Sc | c | 3.891 h | – | – | 0.151 | 0.996 | 2.32 | 4.14 | 4.93 | 5.67 | 5.83 | 5.81 | 4.11 |
| | | | | | (0.019) | (0.100) | (0.20) | (0.43) | (0.47) | (0.56) | (0.55) | (0.56) | (0.41) |
| $^{47}$Ca | c | 4.536 day | – | – | – | – | 0.013 | 0.023 | 0.032 | 0.045 | 0.052 | 0.064 | 0.038 |
| | | | | | | | (0.004) | (0.006) | (0.004) | (0.005) | (0.006) | (0.015) | (0.005) |
| $^{44}$K | c* | 22.13 min | – | – | – | – | – | 0.088 | – | – | 0.185 | – | – |
| | | | | | | | | (0.027) | | | (0.048) | | |
| $^{43}$K | c | 22.3 h | – | – | 0.016 | 0.094 | 0.310 | 0.701 | 1.060 | 1.27 | 1.44 | 1.55 | 1.130 |
| | | | | | (0.003) | (0.009) | (0.024) | (0.067) | (0.090) | (0.12) | (0.12) | (0.14) | (0.100) |
| $^{42}$K | i | 12.360 h | – | – | 0.085 | 0.302 | 1.062 | 2.43 | 3.48 | 4.33 | 4.90 | 4.97 | 3.74 |
| | | | | | (0.009) | (0.029) | (0.080) | (0.24) | (0.31) | (0.40) | (0.43) | (0.45) | (0.35) |
| $^{38}$K | i | 7.636 min | – | – | – | – | 0.098 | 0.421 | 0.696 | 0.88 | 1.03 | 0.91 | 0.75 |
| | | | | | | | (0.025) | (0.069) | (0.091) | (0.12) | (0.15) | (0.18) | (0.10) |
| $^{41}$Ar | c | 109.34 min | – | – | – | 0.024 | 0.097 | 0.288 | 0.463 | 0.645 | 0.809 | 0.858 | 0.653 |
| | | | | | | (0.004) | (0.008) | (0.028) | (0.041) | (0.059) | (0.071) | (0.079) | (0.061) |
| $^{39}$Cl | c | 55.6 min | – | – | – | – | 0.046 | 0.118 | 0.257 | 0.379 | 0.547 | 0.578 | 0.463 |
| | | | | | | | (0.014) | (0.016) | (0.024) | (0.045) | (0.050) | (0.055) | (0.046) |
| $^{38}$Cl | i($m+g$) | 37.24 min | – | – | – | – | – | 0.485 | 0.990 | 1.50 | 1.96 | 2.20 | 1.71 |
| | | | | | | | | (0.056) | (0.093) | (0.14) | (0.18) | (0.22) | (0.16) |
| $^{38}$Cl | c | 37.24 min | – | – | – | – | 0.136 | 0.528 | 1.013 | 1.53 | 2.03 | 2.24 | 1.73 |
| | | | | | | | (0.16) | (0.052) | (0.090) | (0.14) | (0.18) | (0.21) | (0.16) |
| $^{34m}$Cl | i($m$) | 32.00 min | – | – | – | – | 0.038 | 0.157 | 0.406 | 0.685 | 0.990 | 1.080 | 0.881 |
| | | | | | | | (0.023) | (0.019) | (0.037) | (0.065) | (0.090) | (0.100) | (0.084) |
| $^{38}$S | c | 170.3 min | – | – | – | – | – | 0.009 | 0.018 | 0.042 | 0.036 | 0.055 | 0.046 |
| | | | | | | | | (0.017) | (0.020) | (0.006) | (0.005) | (0.009) | (0.006) |
| $^{29}$Al | c | 6.56 min | – | – | – | – | – | 0.093 | 0.525 | 1.05 | 2.09 | 2.18 | 2.32 |
| | | | | | | | | (0.052) | (0.057) | (0.11) | (0.21) | (0.23) | (0.23) |
| $^{28}$Mg | c | 20.915 h | – | – | – | – | 0.004 | 0.016 | 0.059 | 0.122 | 0.271 | 0.381 | 0.380 |
| | | | | | | | (0.004) | (0.001) | (0.005) | (0.011) | (0.024) | (0.035) | (0.035) |
| $^{27}$Mg | c | 9.458 min | – | – | – | – | – | – | 0.232 | 0.525 | 1.034 | 1.34 | 1.38 |
| | | | | | | | | | (0.027) | (0.062) | (0.098) | (0.17) | (0.13) |
| $^{24}$Na | c | 14.9590 h | – | – | – | – | 0.040 | 0.178 | 0.528 | 1.080 | 2.39 | 3.57 | 3.73 |
| | | | | | | | (0.014) | (0.019) | (0.046) | (0.100) | (0.21) | (0.32) | (0.35) |
| $^{22}$Na | c | 2.6019 yr | – | – | – | – | – | 0.120 | 0.423 | 0.769 | 1.70 | 2.56 | 2.75 |
| | | | | | | | | (0.038) | (0.049) | (0.077) | (0.15) | (0.24) | (0.26) |
| $^{7}$Be | i | 53.29 day | 0.137 | 0.206 | 0.271 | 0.329 | 0.873 | 1.29 | 2.38 | 3.54 | 6.05 | 8.33 | 9.07 |
| | | | (0.018) | (0.021) | (0.026) | (0.034) | (0.073) | (0.13) | (0.21) | (0.33) | (0.53) | (0.76) | (0.85) |

**Table 4.** Standard deviations $\langle F \rangle$ for $^{nat}$Cr and $^{56}$Fe

| Model | Sample | Proton energy, MeV | | | | | | | | | | |
|---|---|---|---|---|---|---|---|---|---|---|---|---|
| | | 40 | 70 | 100 | 150 | 250 | 400 | 600 | 800 | 1200 | 1600 | 2600 |
| BERTINI | Cr | 3.54 | 3.06 | 3.27 | 2.42 | 1.86 | 4.39 | 2.82 | 4.14 | 2.96 | 2.63 | 2.26 |
| | Fe | 5.86 | 3.06 | 3.81 | 2.64 | 2.98 | 3.47 | 2.77 | 2.14 | 2.86 | 2.57 | 2.27 |
| ISABEL | Cr | 5.29 | 4.45 | 3.98 | 2.49 | 2.22 | 6.30 | 4.70 | 3.85 | 2.96 | 2.63 | 2.26 |
| | Fe | 4.94 | 5.21 | 6.15 | 3.23 | 2.90 | 3.66 | 5.07 | 4.77 | 2.86 | 2.57 | 2.27 |
| CEM03.02 | Cr | 2.28 | 3.44 | 2.52 | 1.79 | 2.10 | 1.57 | 1.55 | 1.67 | 1.90 | 1.95 | 2.71 |
| | Fe | 3.88 | 3.98 | 2.57 | 2.12 | 2.01 | 2.34 | 1.81 | 1.83 | 1.83 | 1.96 | 2.90 |
| INCL4.2 | Cr | 3.84 | 2.43 | 2.45 | 4.17 | 2.37 | 2.59 | 3.32 | 2.96 | 2.52 | 2.35 | 3.97 |
| | Fe | 3.17 | 3.40 | 5.10 | 3.53 | 3.61 | 4.35 | 5.31 | 6.74 | 3.18 | 3.00 | 3.91 |
| INCL4.5 | Cr | 2.24 | 1.75 | 1.58 | 1.61 | 1.83 | 1.58 | 1.70 | 1.85 | 1.83 | 1.76 | 2.09 |
| | Fe | 2.50 | 3.46 | 1.81 | 1.76 | 2.63 | 2.62 | 1.75 | 1.62 | 1.69 | 1.65 | 2.11 |
| PHITS | Cr | 5.36 | 3.32 | 4.83 | 3.69 | 3.81 | 3.03 | 2.36 | 2.19 | 2.05 | 2.16 | 2.15 |
| | Fe | 2.84 | 5.45 | 4.99 | 4.21 | 3.22 | 3.26 | 2.46 | 2.68 | 2.24 | 2.19 | 2.76 |
| CASCADE07 | Cr | 2.61 | 3.27 | 3.02 | 2.87 | 3.26 | 2.93 | 2.78 | 2.80 | 5.34 | 5.04 | 4.93 |
| | Fe | 5.92 | 4.23 | 3.33 | 2.93 | 3.57 | 3.96 | 3.35 | 3.24 | 5.47 | 4.90 | 4.54 |

0.07, and 0.05 GeV in an extracted beam of the ITEP U-10 synchrotron whose description and parameters are presented in [3, 9]. The method for determining the proton energy on the samples and monitors is described in [2, 3, 9].

The samples were manufactured by pressing of fine-grained powders of iron and chromium and monitors were produced by cutting from an aluminum foil. The diameters of the samples and monitors were 10.5 mm. The samples are made from enriched iron (0.3% $^{54}$Fe, (99.5 $\pm$ 0.1)% $^{56}$Fe, 0.2% $^{57}$Fe, and less than 0.05% $^{58}$Fe) and natural chromium (4.31% $^{50}$Cr, 87.76% $^{52}$Cr, 9.55% $^{53}$Cr, and 2.38% $^{54}$Cr). The total levels of chemical impurities in Cr, Fe, and Al samples were no more than 0.19, 0.00 001 and 0.05%, respectively.

The irradiated targets were sample–monitor "sandwiches" placed into plastic bags [9]. After the complete cycle of the measurements and the analysis of the results, it was found that the presence of the plastic bags under irradiation at the energies of 0.15, 0.1, 0.07, and 0.04 GeV makes an additional contribution to the production of $^{7}$Be in the $^{12}$C$(p, x)^{7}$Be reaction. For this reason, the experimental samples and monitors where additionally irradiated at given energies without plastic bags. The characteristics of the experimental samples and irradiation conditions are presented in Table 1.

After irradiation, the samples and monitors were delivered to a laboratory for subsequent $\gamma$-spectrometric analysis. Two spectrometric channels based on HPGe detectors with the energy resolutions of 1.8 and 1.7 keV for the 1332-keV $\gamma$ line of $^{60}$Co [9] were used as measuring instruments.

The measurements of $\gamma$ spectra continued for 5–7 months after irradiation. The total number of spectra for each sample after 11 irradiation runs was 30–35 and 5–7 for each monitor. The examples of measured $\gamma$ spectra of $^{56}$Fe and $^{nat}$Cr are presented in Figs. 1 and 2. All $\gamma$ spectra of the samples and monitors were processed with the GENIE-2000 program, the interactive fitting mode being mandatorily used. All files obtained for the sample and its monitor were

combined into two independent files, which were used as input files for the SIGMA software package. This package graphically mapped the time changes in the intensity of a chosen $\gamma$ line, which permitted estimating the half-life of the corresponding product. On the basis of the estimated energies and half-lives, product nuclides were identified in accordance with the PPCNUDAT database [10] and the corresponding reaction rates were determined.

The examples of measured and fitted decay curves are presented in Figs. 3 and 4.

## RESULTS AND THEORETICAL PREDICTIONS

The cross sections for radioactive-nuclide production in the $^{56}$Fe$(p, x)$ and $^{nat}$Cr$(p, x)$ reactions induced by 0.04–2.6-GeV protons are presented in Tables 2 and 3. The numbers of measured cross sections $\sigma^{ind}(i)$ and $\sigma^{cum}(c)$ for targets from $^{nat}$Cr and $^{56}$Fe are 302 ($i = 81, i(m+g) = 30, i(m) = 30$, and $c + c^* = 161$) and 347 ($i = 98, i(m+g) = 27, i(m) = 28$, and $c + c^* = 194$), respectively. Using these data, we obtained 33 and 39 excitation functions for $^{nat}$Cr and $^{56}$Fe, respectively; among them, 12 excitation functions for $^{nat}$Cr were measured for the first time.

The average accuracy in determining the cross sections for $^{56}$Fe and $^{nat}$Cr is 11.1 and 10.4%, respectively. The distributions of the uncertainties in the reaction rates and cross sections for nuclide production are presented in Figs. 5 and 6.

The resulting excitation functions were compared with the respective functions calculated by the intranuclear cascade codes BERTINI, ISABEL, CEM03.02, INCL4.2, INCL4.5, CASCADE07, and PHITS [11–17]. The formulas for rescaling the calculated independent cross sections to cumulative ones were given in [3, 8]. Examples of the calculated and experimental excitation functions are shown in Figs. 7 and 8.

The predictive powers of the codes were estimated in terms of the deviation coefficients $\langle F \rangle$ defined as [2, 3]

$$F = 10^{\sqrt{\left\langle \left( \log \frac{\sigma_{exp}}{\sigma_{calc}} \right)^2 \right\rangle}}, \qquad (8)$$

where $\sigma_{exp}$ are the experimental independent or cumulative cross sections and $\sigma_{calc}$ are the independent cross sections obtained with various codes.

The predictive powers of the codes are summarized in Table 4 and Figs. 9 and 10.

## CONCLUSIONS

From a comparison of the calculations with experimental data, it follows that the deviation coefficients $\langle F \rangle$ range from 1.6 to 6.7 for various codes. These values correspond to the deviation of the calculations from the experimental data from 60 to 570%. Such deviations exceed considerably a required accuracy of 30% even for the most accurate code. The discrepancies are particularly large at low energies.

Thus, all intranuclear cascade codes should be further developed. The experimental data obtained in this study can be used both to improve theoretical models and to refine the design of electronuclear facilities and spallation neutron sources.

## ACKNOWLEDGMENTS

This work was supported by the International Science and Technology Center, project no. 3266, and by the State Nuclear Energy Corporation Rosatom.

## REFERENCES

1. A. J. Koning, ECN-C-93-005, ECN-C-93-041 (1993).
2. Yu. E. Titarenko, V. F. Batyaev, E. I. Karpikhin, et al., INDC(CCP)-0434, IAEA (Febr. 2003); http://www-nds.iaea.org/reports-new/indc-reports/indc-ccp/
3. Yu. E. Titarenko, V. F. Batyaev, V. M. Zhivun, et al., INDC(CCP)-0447, IAEA (Oct. 2009); http://www-nds.iaea.org/reports-new/indc-reports/indc-ccp/
4. http://www.istc.ru/istc/db/projects.nsf/All/B212BFCB080126C4C32570AB003166F8?OpenDocument&search=1
5. V. N. Voevodin, VANT, Ser. Fiz. Radiats. Povrezhd. Radiats. Materialoved., No. 2, 10 (2007).
6. Experimental Nuclear Reaction Data (EXFOR) database; http://www-nds.iaea.org/exfor/exfor.htm
7. C. Villagrasa-Canton, A. Boudard, J.-E. Ducret, et al., Phys. Rev. C **75**, 044603-1 (2007).
8. Yu. E. Titarenko, V. F. Batyaev, A. Yu. Titarenko, et al., Phys. Rev. C **78**, 034615 (2008).
9. Yu. E. Titarenko, S. P. Borovlev, M. A. Butko, et al., Yad. Fiz. **74**, 531 (2011, in press).
10. R. Kinsey et al., in *Proceedings of the 9th International Symposium on Capture Gamma Ray Spectroscopy and Related Topics, Budapest, Hungary, 1996*.
11. J. C. Hendricks et al., Report LA-UR-05-2675, LANL (2005); http://mcnp.lanl..gov/
12. S. G. Mashnik and A. J. Sierk, J. Nucl. Sci. Technol. Suppl. **2**, 720 (2002).
13. A. Boudard, J. Cugnon, S. Leray, and C. Volant, Phys. Rev. C **66**, 044615 (2002).
14. J. Cugnon, A. Boudard, S. Leray, et al., ISBN 978-92-0-150410-4, SM/SR-02 (2010).
15. A. R. Junghans et al., Nucl. Phys. A **629**, 635 (1998).

16. H. Iwase et al., J. Nucl. Sci. Technol. **39**, 1142 (2002); http://phits.jaea.go.jp/OvPhysicalModelsJQMD.html
17. H. Kumawat et al., Nucl. Instrum. Methods Phys. Res. B **266**, 604 (2008).
18. R. Michel et al., Nucl. Instrum. Methods Phys. Res. B **129**, 153 (1997); EXFOR, #O0276.
19. R. Michel et al., Nucl. Instrum. Methods Phys. Res. B **103**, 183 (1995); EXFOR, #O0277.
20. R. Michel et al., Nucl. Instrum. Methods Phys. Res. B **16**, 61 (1986); EXFOR, #A0344.
21. R. Michel et al., Analyst **114**, 287 (1989); EXFOR, #O0078016.
22. R. Michel, R. Stueck, and F. Peiffer, *Proton-induced Reaction on Ti, V, Mn, Fe, Co, and Ni Ions*; R. Stueck, PhD Thesis (1983); EXFOR, #A0100007, #A0100008.
23. http://www-nds.iaea.org/exfor/exfor00.htm; EXFOR, #O0729013, #O0728016
24. Th. Schiekel et al., Nucl. Instrum. Methods Phys. Res. B **114**, 91 (1996); EXFOR, #O0284.

*Translated by R. Tyapaev*